ELSEVIER

Catalysis Today 65 (2001) 111–116

CATALYSIS TODAY

www.elsevier.com/locate/cattod

Evidences for pore mouth and key–lock catalysis in hydroisomerization of long *n*-alkanes over 10-ring tubular pore bifunctional zeolites

J.A. Martens [a,*], G. Vanbutsele [a], P.A. Jacobs [a], J. Denayer [b], R. Ocakoglu [b], G. Baron [b], J.A. Muñoz Arroyo [c], J. Thybaut [c], G.B. Marin [c]

[a] *Centrum voor Oppervlaktechemie en Katalyse, KU Leuven, Kardinaal Mercierlaan 92, B-3001 Heverlee, Belgium*
[b] *Chemische Ingenieurstechniek, Vrije Universiteit Brussel, Belgium*
[c] *Laboratorium voor Petrochemische Techniek, Universiteit Gent, Belgium*

Abstract

The evidence for the pore mouth catalysis model for *n*-alkane methylbranching on Pt/H-ZSM-22 hydroisomerization catalyst is reviewed. It is based on adsorption equilibria at catalytic temperatures determined using tracer and perturbation chromatography, reaction product distributions obtained with nC_8–nC_{24} *n*-alkanes and rival model screening for catalytic conversions. In the Henry regime, methylbranched isomers have lower adsorption entropy and enthalpy compared to *n*-alkanes explained by the enhanced rotational and translational freedom of methyl and methylene groups positioned outside the pore interacting with the external surface. Adsorption isotherms for isoalkanes are in agreement with dual site adsorption in pore mouths and on external surfaces, respectively. The hydroisomerization can be modeled with a bifunctional reaction scheme and adsorption on the external crystal surfaces and pore mouths. The selectivity for 2-methylbranching reflects the optimum van der Waals interaction of the *n*-alkane with the zeolite pore and methylbranching in that part of the chain that is located outside the first 10-ring of the zeolite pore to facilitate desorption. Very long *n*-alkanes (C_{12}^+) exhibit key–lock adsorptions and penetrate simultaneously with their two ends into two different pores. Key–lock physisorption leads to branching at more central C atom positions.

Keywords: Pore mouth catalysis; Key–lock catalysis; Hydroisomerization; *n*-Alkanes; ZSM-22

1. Introduction

Controlled skeletal branching of the long *n*-alkane molecules contained in petroleum fractions can be practiced for improving the quality of diesel, aviation fuel and lubricating oils. Properties such as pour point, freezing point, viscosity and viscosity index are significantly improved by introducing side chains along the linear carbon chains. Acid zeolites such as SAPO-11 [1] and ZSM-22 [2] and in their hydrogen form and plated with a trace amount of noble metal are excellent hydroisomerization catalysts for heavy *n*-alkanes, generating high isomerization yields and limited product losses by cracking. These zeolites have tubular pores with quite uniform cross-section delineated by 10-rings of framework oxygen atoms. In these catalysts, the *n*-alkanes undergo preferential methylbranching at the C_2 position [3]. The unique features of the 10-ring tubular pore zeolites were tentatively ascribed by various authors either to pore mouth and

* Corresponding author. Tel.: +32-16-321637; fax: +32-16-321998.
E-mail address: johan.martens@agr.kuleuven.ac.be (J.A. Martens).

0920-5861/01/$ – see front matter
PII: S0920-5861(00)00577-0

key–lock catalysis in pore openings [2,4], transition state shape selectivity [5] or product diffusion selectivity [6–8]. In this paper we present the evidences in favor of pore mouth and key–lock catalysis. For octane hydroisomerization on the Pt/ZSM-22 catalyst, the evidence is based on experimentally determined physisorption equilibria at catalytic temperatures, experimental reaction product distributions obtained with model long *n*-alkane molecules and kinetic models.

2. Alkane adsorption equilibria at low surface coverages

Tracer chromatography was used to determine Henry constants of C_8 alkanes in the temperature range 225–375°C [9]. The temperature dependence of the Henry constant, K' is expressed in the van't Hoff equation

$$K' = K'_0 \, e^{-\Delta H_0/RT} \tag{1}$$

The pre-exponential factor K'_0 of the van't Hoff equation is related to the entropy of adsorption $\Delta S^{\Theta}_{0,\text{local}}$ and the number of adsorption sites n_T [10]

$$K'_0 = \exp\left[\frac{\Delta S^{\Theta}_{0,\text{local}}}{R} + \ln\left(\frac{n_T}{2p^{\Theta}}\right)\right] \tag{2}$$

Henry constants at 300°C, adsorption enthalpies and pre-exponential factors on H-ZSM-22, H-ZSM-5 and H-Beta zeolites are compared in Fig. 1a–c, respectively. On the three zeolites, the Henry constants of methylheptanes are systematically lower than for octane. On H-Beta, the more the methyl group of the methylheptane is positioned in the center of the heptyl chain, the lower is the Henry constant. On H-ZSM-5 and H-ZSM-22, the Henry constants decrease in the same order but the values for $3MC_7$ and $4MC_7$ are identical within experimental error.

For the investigated C_8 alkanes, the pre-exponential factors decrease in the order H-Beta > H-ZSM-5 > H-ZSM-22 (Fig. 1b). This zeolite order parallels the pore width and reflects the lower adsorption entropy in wider pores. The free diameters of the windows in ZSM-22 are $0.44 \times 0.55\,nm^2$. In ZSM-5, there are two types of 10-rings with free apertures of 0.53×0.56 and $0.51 \times 0.55\,nm^2$. The windows of Beta zeolite measure 0.55×0.55 and $0.64 \times 0.76\,nm^2$ [11]. On H-Beta, the K'_0 values decrease slightly in the

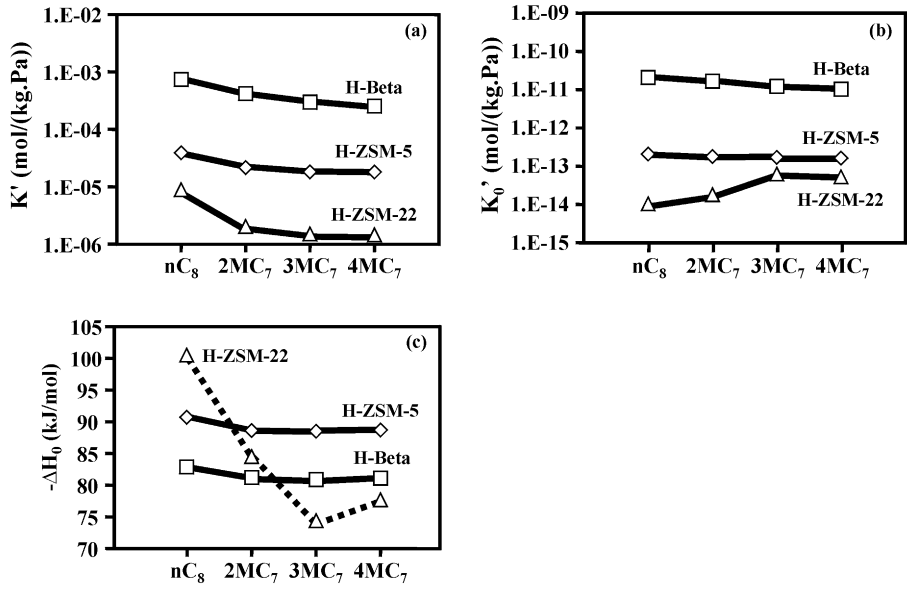

Fig. 1. Henry constant at 300°C (a), pre-exponential factor of van't Hoff equation (b) and adsorption enthalpy at zero coverage (c) of octane and positional methylheptane isomers on H-Beta, H-ZSM-5 and H-ZSM-22 zeolite [9].

order (Fig. 1b)

$$K_0'(n\mathrm{C_8}) > K_0'(2\mathrm{MC_7}) > K_0'(3\mathrm{MC_7}) > K_0'(4\mathrm{MC_7}) \quad (3)$$

This sequence reflects the increase of adsorption entropy in combination with an eventual lower number of adsorption sites with increasing bulkiness of the isomer (Eq. (2)). In H-ZSM-5, the pre-exponential factors for $n\mathrm{C_8}$ and the $\mathrm{MC_7}$ positional isomers are more similar. H-ZSM-22 shows a different K_0' order (Fig. 1b)

$$K_0'(n\mathrm{C_8}) < K_0'(2\mathrm{MC_7}) < K_0'(3\mathrm{MC_7}) = K_0'(4\mathrm{MC_7}) \quad (4)$$

The higher K_0' values for the methylheptanes compared to octane reflect either a larger number of adsorption sites or a smaller adsorption entropy (Eq. (2)). The experimental difference in K_0' for octane and $3\mathrm{MC_7}$ corresponds to 1.8 mmol/g additional adsorption sites for $3\mathrm{MC_7}$. In these tubular pores with uniform diameter the adsorbed *n*-alkanes are aligned on the channel axis and efficiently fill the entire pore. It is difficult to envision a lower number of adsorption sites for $n\mathrm{C_8}$ than for $3\mathrm{MC_7}$. The more likely interpretation is that the order of Eq. (4) reflects the order of adsorption entropies for these molecules. The difference in adsorption entropy of octane and its methylbranched isomers can be explained by the pore mouth adsorption model (Fig. 2). A linear alkyl group penetrates into the pore until the methylbranching reaches the pore entrance. Compared to the *n*-alkane inside the pore, a methylalkane in the pore mouth has a higher rotational and translational freedom, explaining the larger K_0' values. The $3\mathrm{MC_7}$ molecule can adsorb in the pore mouth according to two modes (Fig. 2), leaving either 3 or 5C atoms outside the pore, respectively. This corresponds on an average to 4C atoms outside the pore, which is the same as for $4\mathrm{MC_7}$ explaining the similar K_0'.

The adsorption enthalpy for octane decreases in the order H-ZSM-22 > H-ZSM-5 > H-Beta (Fig. 1c), reflecting the differences in pore diameter and the confinement of the linear alkane in the tubular pore. In H-ZSM-5 and H-Beta, the adsorption enthalpy of octane and methylbranched isomers differs by few kJ/mol only. On H-ZSM-22, the differences are much

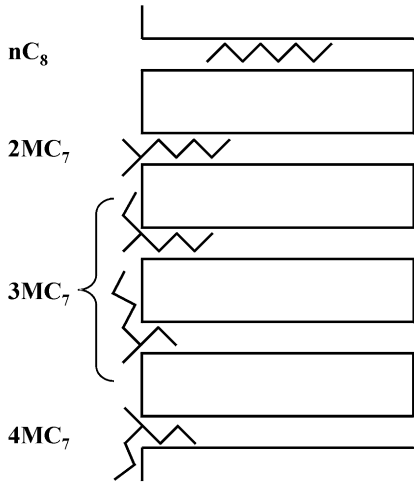

Fig. 2. Schematic representation of intracrystalline adsorption of $n\mathrm{C_8}$ and pore mouth adsorption of methylheptane positional isomers on H-ZSM-22.

larger, viz. ca. +16 kJ/mol between $n\mathrm{C_8}$ and $2\mathrm{MC_7}$, and ca. +10 kJ/mol between $2\mathrm{MC_7}$ and $3\mathrm{MC_7}$. The adsorption enthalpy of $3\mathrm{MC_7}$ and $4\mathrm{MC_7}$ are similar. Although on H-ZSM-22 the adsorption enthalpies of the $\mathrm{MC_7}$ isomers are much smaller than for $n\mathrm{C_8}$, the values are not much lower than in H-Beta, indicating that there is an interaction with the intracrystalline force field. A systematic study of the adsorption of 2-methylbranched isoalkanes with carbon numbers 5–8 revealed that the adsorption enthalpy increases with 11.5 kJ/mol per additional carbon atom in the linear chain [9], similar to the 12.2 kJ/mol increments for the *n*-alkanes [12].

The pore mouth model offers an explanation for the detailed differences in adsorption behavior of the $\mathrm{C_8}$ isomers. Compared to octane, the $2\mathrm{MC_7}$ molecule has 2C atoms less inside the pore interacting with the lower forcefield of the external surface of the zeolite crystal. The adsorption enthalpy of $2\mathrm{MC_7}$ is −85 kJ/mol and situated between that of $n\mathrm{C_6}$ (−75 kJ/mol) and $n\mathrm{C_7}$ (−88 kJ/mol) [12]. The interaction of the two methyl groups of $2\mathrm{MC_7}$ with the external surface accounts for the −10 kJ/mol additional adsorption enthalpy compared to hexane, or −5 kJ/mol per C atom. The adsorption enthalpy for $3\mathrm{MC_7}$ adsorption with 3C atoms outside the pore is estimated at −77 kJ/mol, composed of the enthalpy for pentane (−62 kJ/mol) [12] and −15 kJ/mol contri-

bution from the 3C atoms interacting with the external surface. The adsorption enthalpy for the second possibility of $3MC_7$ adsorption is estimated at −63 kJ/mol, obtained by addition of the enthalpy for 5C atoms on the external surface (−25 kJ/mol) to the adsorption enthalpy of propane (−38 kJ/mol) [12]. The experimental value of −74 kJ/mol is in between these values and closer to the first possibility with the highest number of C atoms inside the pore. For $4MC_7$ there is only one adsorption mode, with 4C atoms inside and 4C atoms outside the pore (Fig. 2) and with adsorption energy roughly estimated at −71 kJ/mol, compared to −78 kJ/mol experimentally. It is concluded that the adsorption entropy and enthalpy values on H-ZSM-22 are in agreement with pore mouth adsorption.

3. Alkane adsorption isotherms on H-ZSM-22

Adsorption isotherms of nC_8 and $2MC_7$ on H-ZSM-22 at 233°C obtained using perturbation chromatography are shown in Fig. 3. The adsorption capacity of $2MC_7$ is strongly reduced compared to nC_8. The adsorption isotherms fit a bi-Langmuir model (Table 1). The nC_8 molecules fill the pores and the external surface, representing 80 m^2/g as determined with N_2 adsorption. $2MC_7$ fills the pore mouths and the external surface (Table 1, Fig. 4). The differences in adsorption constants (K'_{ext} and L_{ext}) between nC_8 and $2MC_7$ are much less pronounced on the external surface than in the pores and pore mouths (K'_{pore} and L_{pore}). Less sterical constraints are imposed on the molecules upon adsorption on the external surface.

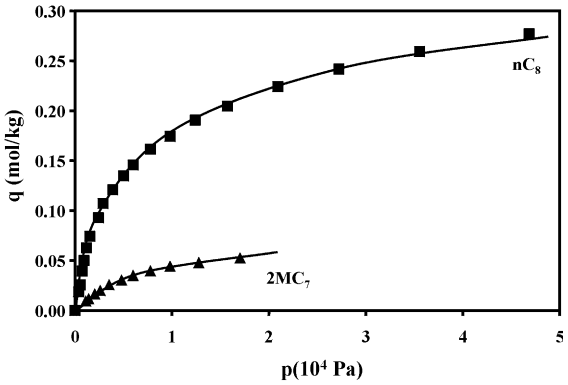

Fig. 3. Adsorption isotherms at 233°C of nC_8 and $2MC_7$ on H-ZSM-22 fitted with bi-Langmuir model (Table 1) [13].

4. *n*-Alkanes hydroisomerization on Pt/H-ZSM-22

The Pt/H-ZSM-22 catalyst contains 0.3 wt.% platinum with an exposed fraction of 46% [3]. The platinum is mostly present on the external surface as observed with TEM. The H-ZSM-22 micropores have homogeneous chemical composition corresponding to an Si/Al ratio of 30 determined by chemical analysis and XPS. There is one acid site every three 10-rings delineating the pores, or every 0.45 nm along the pore.

On Pt/H-ZSM-22 up to medium conversion levels, *n*-alkanes undergo selectively one methyl branching. The positional selectivity of methylbranching of nC_8, nC_{10}, nC_{14}, nC_{18}, nC_{22} and nC_{24} at 25–30% hydroisomerization conversion is shown in Fig. 5. Methylbranching at C_2 is always preferred.

Table 1
Adsorption parameters on H-ZSM-22 at 233°C, derived from fitting with bi-Langmuir model[a] of experimental isotherms determined with perturbation chromatography [13]

	K'_{pore} (mol/kg Pa)[b]	K'_{ext} (mol/kg Pa)	L_{pore} (1/Pa)[c]	L_{ext} (1/Pa)[c]	q^{sat}_{pore} (mol/kg)[d]	q^{sat}_{ext} (mol/kg)[d]
nC_8	11.80×10^{-5}	1.30×10^{-5}	107×10^{-5}	5.8×10^{-5}	0.11	0.22
$2MC_7$	1.84×10^{-5}	1.26×10^{-5}	5412×10^{-5}	17.5×10^{-5}	34×10^{-5}[e]	0.07

[a] $q(p,T) = (K'_{pore}p/(1+L_{pore}p)) + (K'_{ext}p/(1+L_{ext}p))$.
[b] From tracer chromatography.
[c] Langmuir constant.
[d] Saturation capacity.
[e] Estimated from crystal size and morphology.

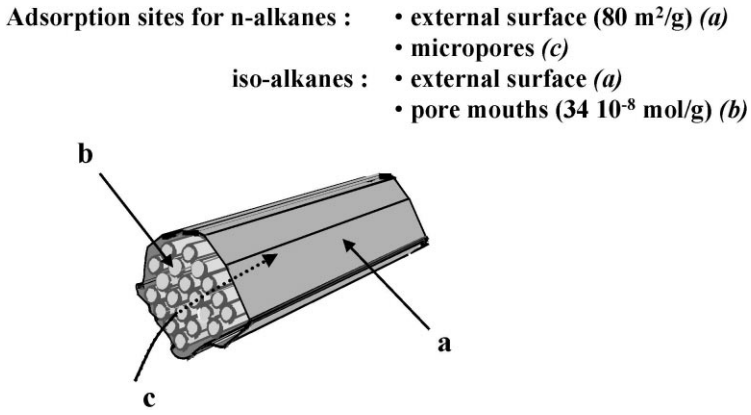

Fig. 4. Adsorption sites on H-ZSM-22 zeolite.

From the adsorption studies (Figs. 1–4, Table 1), it was concluded that at reaction temperature and in a time scale of minutes, methylheptanes including the preferred $2MC_{n-1}$ isomers do not diffuse into H-ZSM-22 crystals. Their tertiary C atom does not pass the window and adsorption occurs in the pore mouth. Considering that the contact time in the reactor is of the order of seconds, diffusion out of the pore of methylbranched skeletal isomerization products from *n*-alkanes formed inside the pore is a very slow process making an insignificant contribution to the catalytic turnovers.

The conversion of nC_8 on Pt/H-ZSM-22 at 233°C was modeled using a lumped reaction scheme and considering the experimentally determined adsorption equilibria in pores, pore mouths and on the external

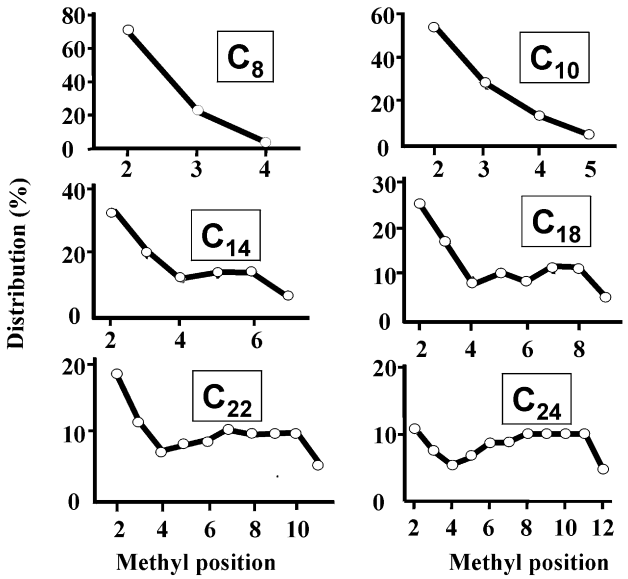

Fig. 5. Distribution (mol.%) of methylalkane isomers obtained at 25–30% hydroisomerization conversion of *n*-alkanes on Pt/H-ZSM-22. $T = 233°C$, $P_{H_2}/P_{HC} = 13.1$ [3].

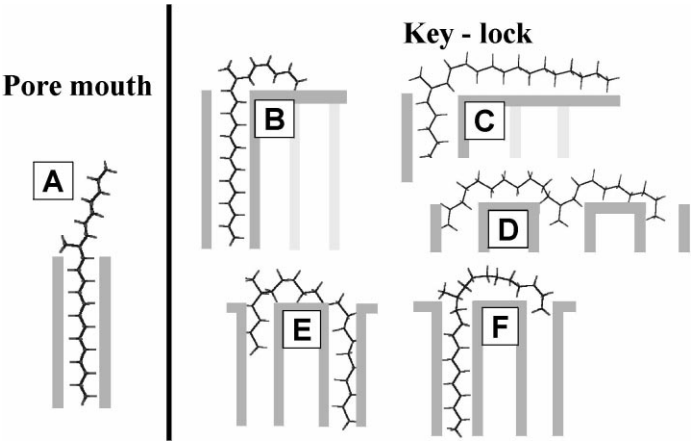

Fig. 6. Favorable adsorption configurations of MC_{21} molecules on ZSM-22 [3].

surface in rival models [13]. Best agreement between model and experiment was reached with the external surface concentrations.

The *n*-alkane on the external surface is dehydrogenated by platinum, enters the pore and optimizes its van der Waals interaction. It undergoes protonation and skeletal branching. The condition for facile desorption is that the branching is generated at the outside of the first 10-ring restriction of the pore. It explains why the formation of a branching is favored at the terminal position of the chain as for this position, the alkane has the largest number of C atoms inside the pore and reaches the highest adsorption potential. The formation of branchings more to the center of the chain involves less favorable physisorption with less C atoms in the pore (Fig. 2).

In the distribution of methylbranched hydroisomerization products from *n*-alkanes (Fig. 5) there is a second broad maximum at methyl positions C_5–C_{11}, depending on carbon number. This second maximum is more developed the longer the *n*-alkane. The formation of these specific more centrally methylbranched isomers can be explained by physisorptions in which the two ends of the alkane penetrate each into a different pore mouth, designated as key–lock adsorptions [2,3] (Fig. 6). Key–lock adsorption and reaction is favored with long molecules [3], at high reaction temperatures [3] and in reactions in the liquid phase [14], where the pores are entirely filled with *n*-alkane molecules present in the feed.

Acknowledgements

This work was sponsored by the Belgian Government through the IUAP-PAI programme.

References

[1] S.J. Miller, Microporous Mater. 2 (1994) 439.
[2] J.A. Martens, W. Souverijns, W. Verrelst, R. Parton, G.F. Froment, P.A. Jacobs, Angew. Chem. Int. Edit. Engl. 34 (1995) 2528.
[3] M.C. Claude, J.A. Martens, J. Catal. 190 (2000) 39.
[4] R. Parton, L. Uytterhoeven, J.A. Martens, P.A. Jacobs, G.F. Froment, Appl. Catal. 76 (1991) 131.
[5] P. Mériaudeau, A. Vu Tuan, G. Sapaly, V.T. Nghiem, C. Naccache, Catal. Today 49 (1999) 287.
[6] E.B. Webb, G.S. Grest, Catal. Lett. 56 (1998) 95.
[7] E.B. Webb, G.S. Grest, M. Mondello, J. Phys. Chem. B 103 (1999) 4949.
[8] Th.L.M. Maesen, M. Schenk, T.J.H. Vlugt, J.P. de Jonge, B. Smit, J. Catal. 188 (1999) 403.
[9] J.F.M. Denayer, G.V. Baron, W. Souverijns, J.A. Martens, P.A. Jacobs, J. Phys. Chem. B 102 (1998) 4588.
[10] J.H. de Boer, S. Kruyer, Entropy and mobility of adsorbed molecules. I. Procedure, atomic gas on charcoal, Proc. Kon. Ned. Akad. Wet. 56 (1952) 451.
[11] W.M. Meier, D.H. Olson, Ch. Baerlocher, Zeolites 17 (1996) 1.
[12] J.F.M. Denayer, G.V. Baron, P.A. Jacobs, J.A. Martens, J. Phys. Chem. B 102 (1998) 3077.
[13] J.F. Denayer, G.V. Baron, G. Vanbutsele, P.A. Jacobs, J.A. Martens, Chem. Eng. Sci. 54 (1999) 3553.
[14] J.A. Muñoz Arroyo, G.G. Martens, G.F. Froment, G.B. Marin, P.A. Jacobs, J.A. Martens, Appl. Catal. A 192 (2000) 9.